Dynamic contrast-enhanced magnetic resonance imaging quantification of leukemia-induced changes in bone marrow vascular function

In this study we show that dynamic contrast enhanced (DCE) magnetic resonance imaging (MRI) can quantify the impact of human acute myeloid leukemia (AML) on bone marrow (BM) vasculature by optimizing an *in vivo* DCE-MRI method and assessing the method's diagnostic and prognostic potential.

AML, the most common acute leukemia in adults,[1] is a very heterogeneous disease with regard to both its genetic basis and outcome of treatment. The BM microenvironment is important because leukemia cells are able to change the functions of normal tissues, favoring proliferation of the cells and protecting them from external harm.[2-4] BM vascular remodeling induced by AML cells favors a more hypoxic microenvironment,[4] and is thought to protect leukemia stem cells from therapy, being a poor prognostic factor in AML.[5,6] Most preclinical studies use microscopy-based methods to assess environmental changes, namely vascular leakiness and perfusion,[7,8] leaving little space for direct translation of the optimized methodology. In the clinic, perfusion imaging is an important tool in the diagnosis and management of various diseases. The advantages of using MRI for perfusion imaging are its superiority in terms of soft tissue contrast, absence of ionizing radiation (compared to computerized tomography and nuclear imaging such as positron emission tomography and single photon emission computed tomography) and the possibility of imaging larger body areas or even the whole body. DCE-MRI is a method commonly used to measure perfusion.[9] DCE-MRI quantifies signal changes due to the passing of a contrast agent through the imaging area. By modeling the signal kinetics, it is possible to quantify vascular parameters such as perfusion, leakiness, and blood volume. Even though it has been around for over 20 years, DCE-MRI has not yet been fully implemented in many clinical pathways because of the lack of standardization in image acquisition and analysis methods, rendering it mostly a research-based tool.

We used DCE-MRI to quantify the impact of human AML on BM vasculature in an animal model. In-house MatLab scripts were used to quantify non-model-based parameters taken directly from the contrast agent kinetic curves (see below). The parameters quantified are illustrated in Figure 1A. Changes in the first part of the DCE curve reflect blood flow and blood volume, while changes in the second part of the DCE curve reflect changes in vascular permeability and extravascular space (Figure 1A).[9]

We have previously reported that leukemia induces BM vascular leakiness, using intravital imaging of the calvaria,[4] which was not observed in mice injected with cord blood (*Online Supplementary Figure S1A, B*), when compared to healthy, age-matched mice that were not injected (NI). To test the sensitivity of DCE-MRI in quantifying leukemia-induced BM vascular dysfunction, three different leukemia cell lines were used (U937, HL60, and ML1), and mice were scanned at different stages of the disease (*Online Supplementary Figure S1C*). When compared to healthy, age-matched NI controls, leukemia mice showed altered BM DCE kinetics (Figure 1B), with reduced contrast enhancement (CE; BM vascular density), reduced wash-in rate (WiR; blood flow), increased initial wash-out rate and wash-out rate (iWoR and WoR; vascular permeability and extravascular space) (Figure 1C). BM vascular dysfunction was not dependent on high leukemia burden, as even low levels of leukemia engraftment (<20% $mCD45^{-}hCD33^{+}$ cells present in the BM) significantly altered BM vascular function (Figure 1C, open circles). Leukemia is known to promote angiogenesis, but with disorganized and leaky vessels.[2,4,10] The reduced CE in our leukemia cohort is in agreement with this, as CE relates to the proportion of functional blood vessels per pixel. With deregulated BM vascular parameters correlating with aging in healthy mice (*Online Supplementary Figure S1D*), we compared younger (12-16 weeks) *versus* older (19-32 weeks) mice to understand whether age was affecting leukemia-induced BM vascular dysfunction. As shown in *Online Supplementary Figure S1D*, older, NI mice showed significantly reduced BM vascular density and increased BM vascular permeability, but we observed no effect of age in leukemia-injected mice (Figure 1C). This indicates that aging and leukemia seem to alter BM vascular permeability (WoR) and functional density (CE) to a similar extent. However, decreased BM blood flow/perfusion (WiR) seems to be a leukemia-specific effect, as it was the only parameter unaltered by aging (*Online Supplementary Figure S1E*). In fact, receiver operating characteristic (ROC) analysis highlighted WiR as the best parameter for distinguishing healthy from leukemic BM (Figure 1D; $AUC_{WiR} = 1.000$).

Differences in vascular density and function between different areas of the bone have been reported.[3] Using intravital two-photon imaging of the calvaria, we confirmed that at early stages of the disease the areas of leukemia engraftment (GFP^{+} cells) coincided with areas of reduced perfusion and irregular vessel structure, confirming a heterogeneous vascular dysfunction linked with leukemia burden (*Online Supplementary Figure S1F*). For this reason, we hypothesize that averaged DCE-MRI parameters could have some limitations in heterogeneous and low-engrafted mice. To obtain a detailed picture of DCE-MRI-measured vascular aberrations and evaluate their spatial distribution along the femur, we performed pixel-by-pixel (pbp, with each pixel corresponding to an area of ~200 μm) analysis for three DCE-MRI parameters: CE, WiR, and WoR. NI mice present a homogeneous distribution of functional vessels in the epiphysis and along the endosteum of the diaphysis (Figure 1E, CE); high vascular perfusion in the central marrow of the diaphysis (Figure 1E, WiR), and higher vascular permeability at the epiphysis and in proximity with the endosteum of the diaphysis. In the presence of AML, there is an aberrant, heterogeneous distribution of these parameters along the femur. In groups injected with HL60 and ML1, pbp analysis highlighted areas (pockets) with severe vascular dysfunction (Figure 1E, white rectangles), surrounded by less affected vasculature. Importantly, areas that showed lower functional vascular density (low CE) corresponded to areas in which both the vascular perfusion (WiR) and permeability (WoR) were mostly affected (Figure 1E, white rectangles). In the group injected with U937 cells, there were no obvious pockets of vascular dysfunction, with this being present throughout the femur. Thus, our pbp analysis approach was successful in resolving the spatial distribution of vascular parameters along the femur and unveiling the heterogeneity of vascular dysfunction in AML xenografts.

To further test the clinical potential of BM DCE-MRI, we scanned mice engrafted with samples from AML patients (i.e., with patient-derived xenografts, PDX). Different AML samples had different engraftment capacities (*Online Supplementary Figure S2A*) and DCE kinetics (Figure 2A), echoing the heterogeneous nature of this dis-

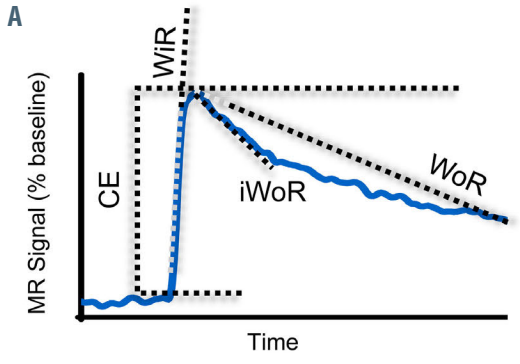

Parameters	Related to
CE: Contrast Enhancement	Functional vascular density
WiR: Wash-in Rate	Blood inflow/velocity; perfusion
WoR: Wash-out Rate	Tissue clearance capacity; permeability
iWoR: initial Wash-out Rate	Same as above, but shorter time frame

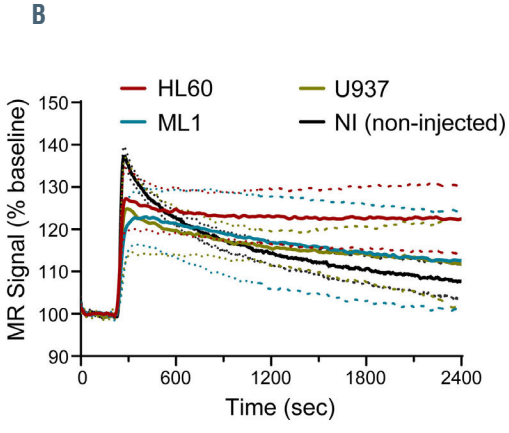

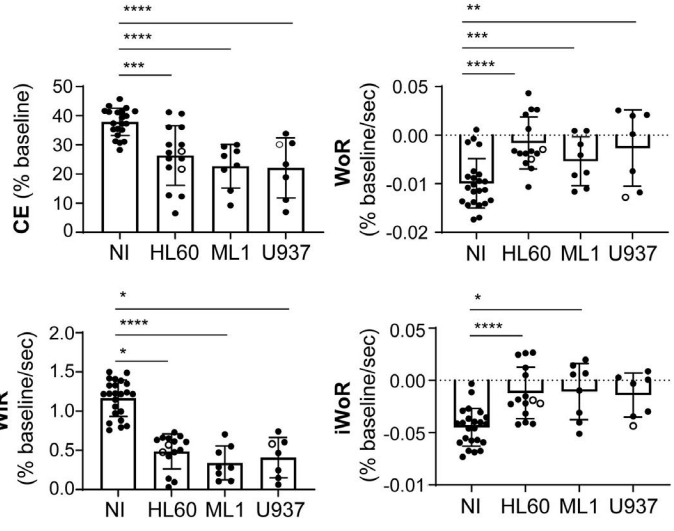

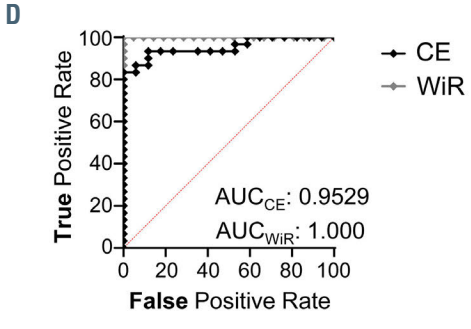

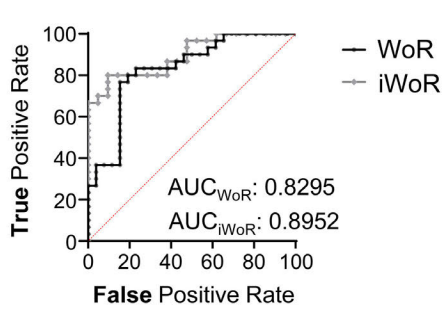

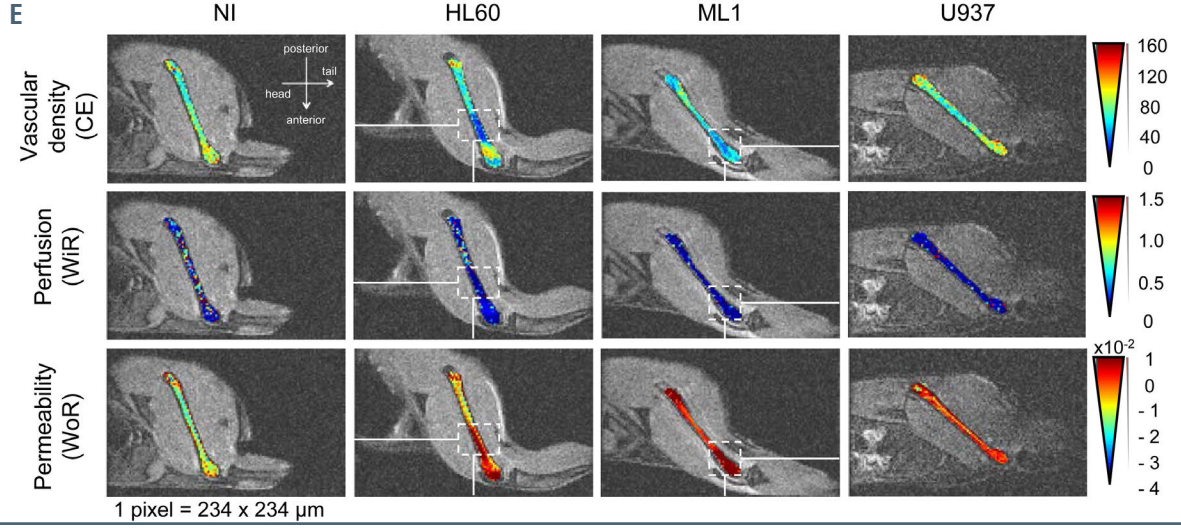

Figure 1. Legend on following page.

Figure 1. Bone marrow vascular changes in aging and leukemia cell line models, measured by dynamic contrast enhanced magnetic resonance imaging. (A) Schematic representation of a dynamic contrast enhanced magnetic resonance imaging (DCE-MRI) time intensity curve and the parameters measured. The table explains what each parameter relates to. (B) Bone marrow (BM) DCE-MRI time intensity curves of non-injected mice (black), mice injected with HL60 (red), ML1 (blue) or U937 (olive green). (C) Quantification of BM DCE-MRI parameters CE, WIR, WoR, and iWoR in non-injected mice (NI) and mice injected with either HL60, ML1 and U937. White circles represent mice with a leukemia burden <20%. Each dot represents one mouse. White columns represent the average of the group and error bars represent the standard deviation of the mean. (D) Receiver operating characteristic analysis of the diagnostic capabilities of the BM DCE-MRI parameters to distinguish malignant from non-malignant BM in the cell line model. (E) Pixel by pixel analysis of BM DCE-MRI parameters showing leukemia-induced changes to the BM tissue. For the HL60 and ML1 groups, white rectangles represent the same area in the BM. MR: magnetic resonance; NI: not injected: AUC: area under the curve; CE: contrast enhancement; WiR: wash-in rate; WoR: wash-out rate; iWoR: initial wash-out rate; *P<0.05; **P<0.01; ***P<0.001; ****P<0.0001.

ease. Mice injected with AML1 had the highest degree of vascular dysfunction (Figure 2A, B), which could also be seen in the pbp analysis (Figure 2C, AML1). Mice from the remaining AML PDX experiments showed no significant changes in CE or WoR, when compared to age-matched controls (old NI mice), similarly to the results from the experiments with AML cell lines (*Online Supplementary Figure S1E*). However, grafts from all the AML patients induced a significant deregulation of the four DCE-MRI parameters compared to those in young NI controls (Figure 2B). As hypothesized, averaged DCE-MRI vascular parameters were not sensitive enough to detect altered BM vasculature in the AML PDX model of low disease burden (<20% $hCD33^+$ cells present in the BM) (Figure 2B, open circles), a limitation that we were able to overcome with pbp analysis (detailed below). Our data highlight the heterogeneous nature of the primary disease compared to cell line models. However, regardless of the broad spectrum of vascular dysfunction, the reduction in BM vascular perfusion (WiR) was again the most significantly affected parameter (Figure 2B) in AML PDX, with ROC curve analysis showing that WiR is of clinical relevance in distinguishing normal from leukemic BM (*Online Supplementary Figure S2B*).

To determine whether DCE-MRI could be used to monitor the BM vascular response to chemotherapy, PDX cohorts were treated with a standard chemotherapy protocol and analyzed during the remission phase. Although cytarabine significantly reduced leukemia burden (*Online Supplementary Figure S2C*), it did not rescue the altered BM vascular phenotype. BM vascular response to cytarabine treatment was diverse, with some groups showing partial rescue (AML1, AML2), and other groups showing no effect at all (*Online Supplementary Figure S2D*).

Pbp analysis showed that vascular dysfunction in some AML samples was located in the whole or most of the diaphysis (AML1, AML3), while in others it was located in small pockets (AML2). Mice injected with sample AML1 exhibited severe BM vascular dysfunction throughout the whole diaphysis, with hardly any perfused pixels (Figure 2C). Cytarabine treatment partly rescued the lack of vascularity in the diaphysis but could not rescue either the vascular perfusion or permeability (Figure 2C, AML1). Even though AML3 did respond to cytarabine treatment (*Online Supplementary Figure S2C*), it showed great similarities with AML1 in terms of most of the vasculature in the diaphysis being compromised, with little to no perfused pixels corresponding to high vascular permeability areas (Figure 2C, AML3). AML4 and AML5 showed similar patterns of pixel distribution. Before therapy, both AML samples showed a modest effect on BM vasculature, and for both samples, cytarabine treatment seemed to worsen the phenotype for both perfusion and permeability (Figure 2C, AML4 and AML5).

Imaging the microenvironment can provide important insights and has diagnostic power.[11,12] In leukemia, clinical imaging is not part of the routine follow-up of patients, although clinical studies have shown the utility of DCE-MRI.[5,13] Our preclinical imaging data, focusing on femoral BM, sheds some lights on the nature of the vascular microenvironment involvement in AML at diagnosis and during remission, and our in-house image analysis pipeline maximizes the translational potential of the technique, without the need of complex modeling analysis. This strategy resolves the caveats encountered with standard model-based quantification of the parameters, whose clinical relevance depends strongly on the mathematical model chosen.[14] Our results pave the way for the implementation of a novel human BM tailored DCE-MRI model which would help to provide an absolute or correlative biomarker in clinical settings. Among the various parameters analyzed, the WiR has the best diagnostic potential as measured by ROC analysis. This could potentially be helpful in the scenario of long-term disease, patients' refusal to have a bone marrow puncture, or high-risk and/or older patients in whom frequent and thorough follow-up monitoring might be a value. Future clinical investigations will be needed to formally address the utility of this technique.

We were also able to show that vascular dysfunction occurs in healthy aging. Recent reports suggest that a damaged BM niche could have a role in the aging process of the hematopoietic system.[15] High vascular permeability being associated with increased HSC activation and egress from the niche,[8] our data are in line with these findings and point to a possible therapeutic benefit from restoring normal vascular functionality.

All animal experiments in this study were performed under the project license (PPL 70/8904) approved by the UK Home Office and in accordance with the Francis Crick Institute AWERB (Animal Welfare and Ethics Review Board) guidelines. NOD.Cg-*Prkdc*^{scid}*Il2rg*^{tm1Wjl} (NSG) strains were obtained from Jackson Laboratory (Bar Harbor, ME, USA) and were bred in-house.

Cell lines (HL60, ML1, U937) came originally from the American Type Culture Collection (distributor LGC standards, UK) and were grown by our cell service at the Institute. Before use, these lines were authenticated using short tandem repeat profiling. Once authenticated, $2x10^6$ cells per mouse were injected intravenously into NSG mice of different ages. BM engraftment was assessed by FACS analysis of BM aspirate 2-4 weeks after injection. For specific experiments, cell lines were transfected with GFP-Luciferase lentivirus vector, as previously described.[4]

The collection and use of all human samples were approved by the East London Research Ethical Committee (REC:06/Q0604/110) and performed in accordance with the Declaration of Helsinki. Umbilical cord blood samples were obtained from normal full-term deliveries after signed informed consent.

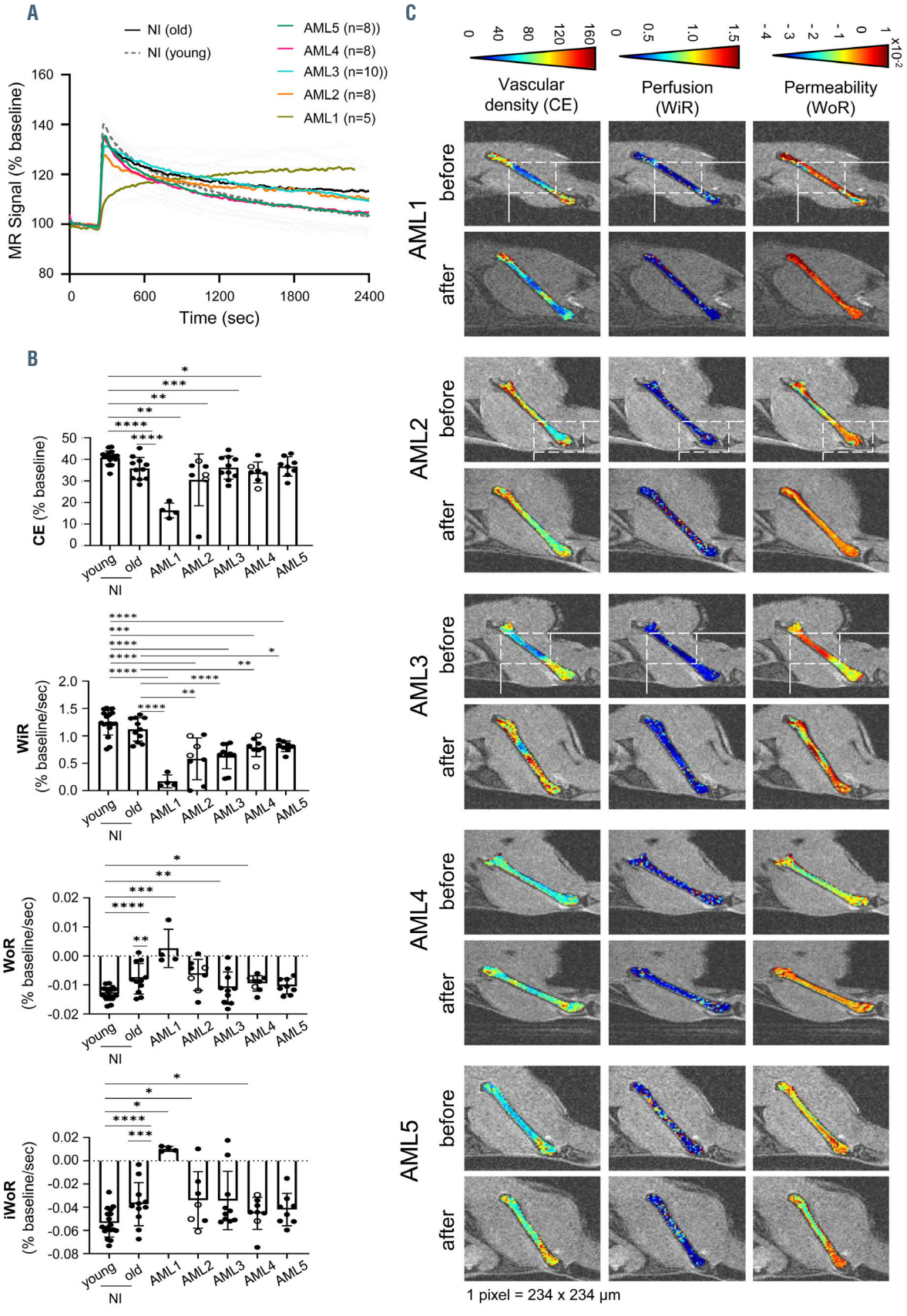

Figure 2. Legend on following page.

Figure 2. Dynamic contrast enhanced magnetic resonance imaging can help to distinguish normal from leukemic bone marrow in acute myeloid leukemia patient-derived xenograft models. (A) Bone marrow (BM) dynamic contrast enhanced magnetic resonance imaging (DCE-MRI) time intensity curves of non-injected young mice (NI, black), non-injected age-matched mice (NI, dashed black) and mice injected with samples from patients 1-5 with acute myeloid leukemia (AML1-AML5). (B) Quantification of the BM DCE-MRI parameters contrast enhancement, wash-in rate, wash-out rate and initial wash-out rate for the mice represented in (A). White circles represent mice with leukemia burden <20%. Each dot represents one mouse. White columns represent the average of the group and error bars represent the standard deviation of the mean. (C) Pixel by pixel analysis of BM DCE-MRI parameters from mice in *Online Supplementary Figure S1F*, showing leukemia-induced changes to the BM tissue. White rectangles represent the same area in the BM for that specific mouse. MR: magnetic resonance; NI: not injected; BM: bone marrow; AML: acute myeloid leukemia; DCE-MRI: dynamic contrast enhanced magnetic resonance imaging; CE: contrast enhancement; WiR: wash-in rate; WoR: wash-out rate; iWoR: initial wash-out rate; **P*<0.05; ***P*<0.01; ****P*<0.001; *****P*<0.0001.

AML samples were obtained after informed consent at St Bartholomew's Hospital (London, UK). T-cell depleted AML samples were injected intravenously into 8- to 12-weeks old unconditioned NSG mice ($2x10^6$ cells per mouse). Ten to 14 weeks after injection, mice were treated with a daily subcutaneous injection of cytarabine (10 mg/kg) for 7 consecutive days. Response to treatment response was assessed 2 weeks after the start of treatment, by flow cytometry analysis of BM aspirates.

At the end of each experiment, animals were euthanized and bone processed as already reported for FACS analysis.[4] The antibodies used were anti-mouse CD45-PerCPCy5 (1:200, eBioscience, #45045182); anti-human CD33-PE (1:100, BD Pharmingen, #555450); anti-human CD45- APC-eFluor 780 (1:100, eBioscience, #47045942). Flow cytometry analysis was performed using a Fortessa flow cytometer (BD Biosciences, Oxford, UK).

For magnetic resonance imaging, mice injected with leukemia cell lines were scanned 2-4 weeks after injection. Mice injected with AML patients' samples were scanned before and after treatment with cytarabine. MRI was performed on a 9.4 T horizontal bore system (Bruker GmbH) equipped with a B-GA12SH gradient coil system. RF transmission and reception were performed with a 40 mm ID quadrature birdcage coil (Bruker GmbH). A series of fast low-angle shot (FLASH) scans were used for femur localization and for slice positioning.

DCE scans were performed using a FLASH with the following parameters: repetition time = 17.639 ms; echo time = 1.859 ms; flip angle = 10°; repetition = 1100; field of view 30x30x0.5 mm^3; matrix 128x128, and resolution of 234 µm. Dotarem (0.4 mL/Kg, Guerbet, France) was injected 4 min after the start of the scan. The total duration of the scan was 41 min. All mice were placed in a head-first prone position for imaging. Anesthesia was induced and maintained using isoflurane (1-4%) in room air supplemented with oxygen (80%/20%). Temperature and respiration rate were monitored using an SA Instruments system (Bayshore, NY, USA).

To assess vascular perfusion in BM vessels by two-photon microscopy, we used a previously described protocol.[4] Images were obtained on a Zeiss 710 NLO laser scanning multiphoton microscope with a 20x 1.0 NA water immersion lens. The bone signal (second harmonic generation) was collected at 380-485 nm; GFP signals from AML cells was collected at 500-550 nm; the signal from Qtracker® 655 Vascular Label was collected at 640-690 nm by not descanned detectors. Each z stack of images (100-150 µM) was rendered in three dimensions using Imaris software (Bitplane).

We used Matlab 2019a for all DCE-MRI image analyes. One region-of-interest (ROI) was drawn for the BM and another for the muscle, per scan, per mouse. The signal in each ROI was then averaged and normalized to its baseline, so that it reflected percentage change from baseline. Signals from frames 3-90 were used as baseline. The muscle ROI was used as the internal control to rule out problems with the injection and/or systemic issues with blood circulation. Mice that showed abnormal DCE muscle kinetics were excluded from the analysis.

Parameters quantified from DCE time intensity curves were CE, WiR, WoR and iWoR. The CE was quantified as the percentage signal difference between baseline and maximum value from frames 95-300. The WiR was determined from the slope of the linear fit between the frame at which CE was reached and the frame at which the signal started to increase. The WoR was determined from the slope of the linear fit between the frame at which CE was reached and the end of the scan. The iWoR was determined from the slope of the linear fit between the frame at which CE was reached and the frame 5 mins later; Pbp analysis was done using the same scripts but applying them to every pixel inside of the bone marrow ROI.

Statistical differences in parameters between mice groups were calculated using two-tailed unpaired *t*-tests. Correlation analysis was done using two-tailed Pearson correlation analysis. ROC curves were calculated using the Wilson/Brown method.

Ana L. Gomes,[1] John Gribben,[2] Bernard Siow,[3#] Diana Passaro[1,4#] and Dominique Bonnet[1#]

[1]Haematopoietic Stem Cell Laboratory, The Francis Crick Institute; [2]Department of Haemato-Oncology, Barts Cancer Institute, Queen Mary University of London and [3]In Vivo Imaging, The Francis Crick Institute, London, UK

[#]BS, DP and DB contributed equally as co-senior authors.

Correspondence:

DOMINIQUE BONNET - dominique.bonnet@crick.ac.uk

DIANA PASSARO - diana.passaro@inserm.fr

BERNARD SIOW - bernard.siow@crick.ac.uk

doi:10.3324/haematol.2020.277269

Received: December 4, 2020.

Accepted: March 18, 2021.

Pre-published: March 25, 2021.

Disclosures: no conflicts of interest to disclose.

Contributions: ALG, DP and DB: wrote the manuscript; ALG, DP and DB designed the experiments; ALG and DP performed experiments and analyzed data; DB and DP secured funding; ALG and BS developed and optimized the MRI protocol; JG provided human AML samples.

Acknowledgments: the authors would like to thank the Biological Research Facility, Flow Cytometry and In Vivo Imaging core facilities at the Francis Crick Institute for their valuable help. The authors are grateful to Prof. John Gribben (St. Bartholomew's Hospital, London, UK) for providing human AML samples.

Funding: ALG was supported by an i2i translational grant scheme

from the Francis Crick Institute. DP was supported by a non-clinical junior research fellowship from the European Hematology Association. This work was supported by The Francis Crick Institute, which receives its core funding from Cancer Research UK (FC001045), The UK Medical Research Council (FC001045), and the Welcome Trust (FC001045).

Data sharing statement: scan data are available upon request. Please contact the corresponding author.

References

1. Sant M, Allemani C, Tereanu C, et al. Incidence of hematologic malignancies in Europe by morphologic subtype: results of the HAEMACARE project. Blood. 2010;116(19):3724-3734.
2. Hanoun M, Zhang D, Mizoguchi T, et al. Acute myelogenous leukemia-induced sympathetic neuropathy promotes malignancy in an altered hematopoietic stem cell niche. Cell Stem Cell. 2014; 15(3):365-375.
3. Duarte D, Hawkins ED, Lo Celso C. The interplay of leukemia cells and the bone marrow microenvironment. Blood. 2018;131(14):1507-1511.
4. Passaro D, Di Tullio A, Abarrategi A, et al. Increased vascular permeability in the bone marrow microenvironment contributes to disease progression and drug response in acute myeloid leukemia. Cancer Cell. 2017;32(3):324-341.
5. Padro T, Ruiz S, Bieker R, et al. Increased angiogenesis in the bone marrow of patients with acute myeloid leukemia. Blood. 2000;95(8):2637-2644.
6. Medyouf H. The microenvironment in human myeloid malignancies: emerging concepts and therapeutic implications. Blood. 2017; 129(12):1617-1626.
7. Bixel MG, Kusumbe AP, Ramasamy SK, et al. Flow dynamics and HSPC homing in bone marrow microvessels. Cell Rep. 2017;18(7): 1804-1816.
8. Itkin T, Gur-Cohen S, Spencer JA, et al. Distinct bone marrow blood vessels differentially regulate haematopoiesis. Nature. 2016; 532 (7599):323-328.
9. Cuenod CA, Balvay D. Perfusion and vascular permeability: basic concepts and measurement in DCE-CT and DCE-MRI. Diagn Interv Imaging. 2013;94(12):1187-1204.
10. Hussong JW, Rodgers GM, Shami PJ. Evidence of increased angiogenesis in patients with acute myeloid leukemia. Blood. 2000; 95(1):309-313.
11. Subashi E, Choudhury KR, Johnson GA. An analysis of the uncertainty and bias in DCE-MRI measurements using the spoiled gradient-recalled echo pulse sequence. Med Phys. 2014;41(3):032301.
12. Cao J, Pickup S, Clendenin C, et al. Dynamic contrast-enhanced MRI detects responses to stroma-directed therapy in mouse models of pancreatic ductal adenocarcinoma. Clin Cancer Res. 2019; 25(7): 2314-2322.
13. Hou HA, Shih TT, Liu CY, et al. Changes in magnetic resonance bone marrow angiogenesis on day 7 after induction chemotherapy can predict outcome of acute myeloid leukemia. Haematologica. 2010; 95(8):1420-1424.
14. Paudyal R, Lu Y, Hatzoglou V, et al. Dynamic contrast-enhanced MRI model selection for predicting tumor aggressiveness in papillary thyroid cancers. NMR Biomed. 2020;33(1):e4166.
15. Lazzari E, Butler JM. The instructive role of the bone marrow niche in aging and leukemia. Curr Stem Cell Rep. 2018;4(4):291-298.